Journal of Translational Medicine

RESEARCH

Open Access

A humanized anti-MSLN×4-1BB bispecific antibody exhibits potent antitumour activity through 4-1BB signaling activation and fc function without systemic toxicity

Da-yan Zhang[1,2,3†], Zhi-hua Zhang[1,3†], Wen-ting Liu[2,3], Wei-ming Zhou[2,3], Peng-fei Zhou[2,3], Juan-juan Wei[2,3], Xue-jing Dai[2,3], Xiao-li Zeng[2,3], Yu-qiong Zhou[2,3], Han-wang Li[2,3], Heng Zhang[2,3], Ao-lin Shen[3,4*], Lian-sheng Cheng[2,3*], Guo-dong Shen[3,5*] and Yi-fu He[1,3*]

Abstract

Background Agonistic monoclonal antibodies targeting 4-1BB/CD137 have shown preclinical promise, but their clinical development has been limited by severe liver toxicity or limited efficacy. Therefore, a safe and efficient immunostimulatory molecule is urgently needed for cancer immunotherapy.

Methods A novel anti-MSLN×4-1BB bispecific antibody (bsAb) was generated via antibody engineering, and its affinity and activity were detected via enzyme-linked immunosorbent assay (ELISA), flow cytometry, and T-cell activation and luciferase reporter assays. In vivo antitumour activity was assessed by establishing humanized mice bearing human MSLN-expressing MC38 (MC38/hMSLN) or CT26 (CT26/hMSLN) cells, and safety was further evaluated in cynomolgus monkeys.

Results We generated two humanized anti-MSLN×4-1BB bsAbs (HK013-G1/G4) by fusing an anti-4-1BB scFv to the C-terminus of an anti-MSLN VHH with an intact Fc fragment from human IgG1 or IgG4. The two bsAbs were able to block the binding of CA125 to MSLN and stimulate 4-1BB signaling pathway, which was strictly dependent on MSLN expression. In particular, HK013-G1 retained Fc function and induced ADCC effect in tumour cells, whereas HK013-G4 did not. Strikingly, HK013-G1 showed superior antitumour activity to HK013-G4 both in vitro and in vivo and remained effective even in the presence of soluble MSLN. HK013-G1 enhanced antitumour immunity and induced

†Da-yan Zhang and Zhi-hua Zhang contributed equally to this work.

*Correspondence:
Ao-lin Shen
shenaolin@ustc.edu.cn
Lian-sheng Cheng
charlson@ustc.edu.cn
Guo-dong Shen
gdshen@ustc.edu.cn
Yi-fu He
yifuhe@ffyy.ustc.edu.cn

Full list of author information is available at the end of the article

durable antigen-specific immune memory to prevent rechallenged tumour growth, even at a dose as low as 1 mg/kg. Furthermore, HK013-G1 did not induce nonspecific production of proinflammatory cytokines and showed good tolerability up to the highest tested dose (30 mg/kg weekly) for 5 weeks, with no HK013-G1-related adverse effects observed in cynomolgus monkeys. In addition, the mean half-life of HK013-G1 was approximately 61 and 97 h at single doses of 3 and 30 mg/kg, respectively.

Conclusion The optimal anti-MSLN×4-1BB bsAb HK013-G1 exhibited synergistic antitumour effects by inducing an ADCC effect (innate immunity) and stimulating the 4-1BB signaling pathway (adaptive immunity) upon cross-bridging with MSLN with no systemic toxicity, which may offer the promise of an improved therapeutic window relative to that of 4-1BB agonists.

Keywords 4-1BB/CD137, MSLN, Bispecific antibody, Cancer immunotherapy, Antitumour immunity

Background

The great success of immune checkpoint inhibitors and T-cell engagers indicates that immunomodulation of the immune system, either via blockade of inhibitory signals or delivery of stimulatory signals, has an important role in cancer therapy [1–3]. 4-1BB, also known as CD137 or tumour necrosis factor receptor superfamily member 9 (TNFRSF9), is an important costimulatory molecule that is expressed on the surface of activated T cells and other immune cells [4, 5]. Binding of 4-1BB to its ligand triggers receptor oligomerization and immune signaling activation, thereby promoting T-cell proliferation and cytokine release and enhancing the cytotoxicity of CD8 + T cells [6]. Although several 4-1BB agonistic agents, including urelumab (BMS-663513), utomilumab (PF-05082566) and ZG033 (HuB6), have entered clinical trials, the problem of serious adverse events (AEs) or low clinical benefit has not been resolved well [7–9].

The bispecific antibody (BsAb) targeting 4-1BB and tumour-associated antigens (TAAs) has the advantage of crosslinking 4-1BB only in the presence of TAAs; thus, this development strategy is highly favored by the pharmaceutical industry [10–12]. Mesothelin (MSLN) is a tumour antigen highly expressed in various human cancers that can activate the NF-κB, MAPK and PI3K pathways and promote cell proliferation and migration and is an attractive target for cancer therapy [13–15].

Here, we developed an anti-MSLN×4-1BB bispecific antibody (bsAb), HK013, by fusing a single-chain variable fragment (scFv) targeting 4-1BB at the C-terminus of an anti-MSLN nanobody and confirmed that HK013 could bridge MSLN-positive and 4-1BB-positive cells, activate the 4-1BB costimulatory pathway and kill tumour cells in a manner dependent on MSLN expression. Moreover, HK013-G1 showed better antitumour efficacy than its IgG4 control HK013-G4, with no signs of toxicity in vitro or in vivo.

Methods

Cell culture

The NCI-H226 (CBP60129), OVCAR3 (CBP60294) and AsPC-1 (CBP60546) human tumour cell lines; the MC38 (CBP60825) and CT26 (CBP61189) murine colorectal cancer cell lines; and the NK92 (CBP60980) cell line were purchased from Cobioer Biosciences (Nanjing, China). The human tumour cell lines were cultured in RPMI-1640 (HyClone) supplemented with 10% fetal bovine serum (FBS, Gibco). NK92 cells were maintained in RPMI 1640 (HyClone) supplemented with 15% FBS, 0.2 mM inositol, 0.02 mM folic acid, and 200 U/ml recombinant IL-2 (Novoprotein Scientific, Inc.). MC38 and CT26 cells were stably transfected to express human MSLN, which were subsequently cultured in RPMI 1640 medium supplemented with 10% FBS, 1% penicillin/streptomycin (P/S, HyClone) and 1 mg/ml geneticin (Gibco). CHO-K1/MSLN cells expressing full-length human MSLN and CHO-K1/4-1BB cells expressing full-length human 4-1BB were generated via lentiviral transduction. CHO-K1/FcγRIIA, CHO-K1/FcγRIIB and CHO-K1/FcγRI cells were designed to express human FcγRIIA, FcγRIIB and FcγRI on the cell membrane, respectively. All of the engineered CHO-K1 cells were cultured in DMEM/F12 (HyClone) supplemented with 10% FBS, 1% P/S and 1 mg/ml geneticin. HEK-293/NFκB-Luci/4-1BB cells were genetically engineered, expressed human 4-1BB and a luciferase reporter driven by NFκB and cultured in DMEM (HyClone) supplemented with 10% FBS, 1% P/S, 1 μg/ml puromycin (Gibco) and 800 μg/ml hygromycin B (Sangon Biotech, Shanghai). FcγRIIIa (158 V) Jurkat effector cells (GM-C05619) were purchased from Genomeditech (Shanghai, China). All the cell lines were cultured at 37 °C in a humidified incubator with 5% CO2.

Protein expression and purification

The amino acid sequences for human MSLN and 4-1BB were obtained from UniProt (https://www.uniprot.org/uniprotkb, MSLN: Q13421, 4-1BB: Q07011), and those for control antibodies, including urelumab (IMGT/mAb-DB, ID: 373) and amatuximab (MORAb-009, IMGT/mAb-DB

ID: 64), were obtained from IMGT/mAb-DB (http://www.imgt.org/mAb-DB). The sequences of the antibodies and the extracellular domains of the target proteins that were fused to the Fc region of the mice or a 6×hexahistidine tag were synthesized, cloned and inserted into the mammalian expression vector pcDNA3.4 TOPO (Invitrogen), followed by transfection into the Expi293F expression system (Gibco) in accordance with the manufacturer's protocols. Proteins were purified via protein A chromatography or Ni^{2+} chromatography (Cytiva) via an AKTA Pure Chromatography System (GE Healthcare). Size exclusion chromatography over a Superdex 200 10/60 PG column (GE Healthcare) for antibodies was implemented for further purification.

Enzyme-linked immunosorbent assay (ELISA)

Recombinant human MSLN-His or 4-1BB-mFc was dissolved in 0.5 M $NaHCO_3$ at 1 μg/mL and coated into the wells of a Nunc Maxisorp plate. After being incubated overnight at 4 °C and washed three times with PBS containing 0.05% (v/v) Tween 20 (PBST), the 96-well plate was blocked with 5% (w/v) milk in PBST at 37 °C for 2 h. After washing with PBST, the plate was incubated with 4-fold serial dilutions of HK013-G1, HK013-G4, αMSLN or α4-1BB parental protein in 1% (w/v) milk in PBST at 37 °C for 1 h and then washed three times with PBST. The plate was incubated with anti-human Fc-HRP (Jackson), which was diluted 6000-fold with 1% (w/v) milk in PBST, for 30 min. After washing with PBST, 50 μL of TMB (Thermo Scientific™) and H_2SO_4 (stop solution) were sequentially added to each well. Optical density was measured at 450 nm using VersaMax (Molecular Devices). All tests were conducted in duplicate.

For the CA125/MSLN blockade assay, a Nunc Maxisorp plate was coated with 5 μg/mL recombinant human CA125-His (Kactus Biosystems) in carbonate buffer at 4 °C overnight. After blocking and washing, the plate was incubated with 5 nM human MSLN-mFc and 10-fold serial dilutions of the HK013-G1, HK013-G4 or αMSLN parental protein at 37 °C for 1 h. After being washed three times with PBST, the plate was incubated with anti-mouse Fc-HRP (Jackson) for 30 min. After washing, 50 μL of TMB (Thermo Scientific™) and H_2SO_4 (stop solution) were sequentially added to each well. Optical density was measured at 450 nm using VersaMax (Molecular Devices). All tests were conducted in duplicate.

Flow cytometric analysis

For flow cytometry, we used high MSLN-expressing human lung squamous cell carcinoma (NCI-H226), moderate MSLN-expressing human ovarian carcinoma (OVCAR3) and low MSLN-expressing human pancreas adenocarcinoma (AsPC-1) samples. A total of 2×10^5 cells were placed in PBS containing 1% BSA and incubated with 2-fold serially diluted HK013-G1, HK013-G4, αMSLN or α4-1BB parental protein for 1 h at 4 °C. After being washed with suspension buffer, the cells were incubated for 30 min at 4 °C with APC-labeled antibodies against human IgG (Jackson). The cells were subsequently washed, resuspended in 400 μL of PBS containing 2% BSA, and subjected to flow cytometric analysis via a CytoFlex analyzer (Beckman Coulter).

To determine the mechanism of cobinding by HK013-G1, CHO-K1-h4-1BB cells stained with CFSE (5,6-carboxyfluorescein diacetate, succinimidyl ester; Invitrogen) were cocultured with CHO-K1-hMSLN cells labeled with the cell tracker Deep Red (C34565; Thermo Fisher) at a ratio of 1:1 with specified concentrations of the tested antibodies for 1 h in a 96-well plate. The percentage of cobinding cells that were double positive was analyzed via the CytoFlex system.

CD8 + T-cell activation assay

Human primary CD8 + T cells were isolated from PBMCs via a kit (557766, BD). To test 4-1BB agonist activity, 2×10^4 CHO-K1-hPD-L1 or CHO-K1 cells were seeded into 96-well plates precoated with 0.5 μg/mL anti-CD3 (BioLegend). After the cells were incubated overnight and treated with 20 μg/mL mitomycin (Energy Chemical) for 3.5 h, the supernatant was aspirated, and 2×10^4 CD8 + T cells and serially diluted HK013-G1 or other antibodies were added to each well and incubated in a CO2 incubator at 37 °C. After 3 days, the concentration of IFN-γ in the cell supernatant was measured via ELISA.

NF-κB luciferase reporter assay

To confirm the effect of 4-1BB stimulation by HK013-G1, an NFκB luciferase reporter gene assay was used with different MC38/MSLN cells with different MSLN expression levels. HEK-293/NFκB-Luci/4-1BB cells were seeded at 1.5×10^4 cells per well in a 96-well plate (Corning). Then, different MC38/MSLN cells with high, moderate and low MSLN expression were added at 1.5×10^4 cells per well. Serially diluted HK013-G1, HK013-G4, urelumab or the parental protein α4-1BB was cocultured with the cells in a CO2 incubator at 37 °C for 18 h. Next, an equal volume of firefly luciferase reagent was added, and the luciferase activity was analyzed via a SpectraMax (Molecular Devices).

To investigate the ability of HK013-G1 to induce 4-1BB signaling activity in the presence of FcγR cross-linking, HEK-293/NFκB-Luci/4-1BB cells and CHO-K1 cells with different FcγR expression levels (CHO-K1/FcγRI, CHO-K1/FcγRIIA, and CHO-K1/FcγRIIB cells) were seeded in a 96-well plate and incubated with HK013-G1 and other antibodies overnight in a CO2 incubator at 37 °C.

Cytotoxicity assay

To test the antibody-dependent cell-mediated cytotoxicity (ADCC) mediated by HK013, ADCC effector cells (FcγRIIIa Jurkat effector cells, 3×10^4 cells/well) and target cells (OVCAR3 cells, 3×10^4 cells/well) were seeded in 96-well plates. Serially diluted HK013 or control antibody was added, and the samples were incubated at 37 °C with 5% CO2 for 18 h. Luminescence was detected by a SpectraMax following the addition of an equal volume of firefly luciferase reagent.

HK013-induced NK cell activity was tested in MSLN-expressing human cancer cells via an LDH assay (Dojindo). The procedures were performed in accordance with the manufacturer's protocol. Briefly, NK92 cells and target cells were seeded in each well at an E: T ratio of 5:1, and serially diluted HK013 was added. HEK293 cells were used as negative controls. After the mixture was incubated at 37 °C and 5% CO2 for 3.5 h, 20 μL of lysis solution was added, and the mixture was incubated for 30 min. Next, 50 μL of the supernatant was transferred to a 96-well plate, and 50 μL of LDH working solution was added to each well. The plate was incubated at room temperature for 30 min in the dark, after which 50 μL of stop solution was added. The optical density (OD) was measured at a wavelength of 490 nm (Microplate reader, Versa Max).

HK013-mediated cytotoxicity in MSLN-expressing cancer cells in PBMCs was detected via calcein retention according to the manufacturer's instructions (Yeasen, Shanghai). NCI-H226, OVCAR3 or AsPC-1 target cells were incubated with 10 μM calcein-AM in complete medium for 30 min at 37 °C. After two washes with complete medium, calcein-AM-labeled target cells (1×10^4 cells/well) were seeded together with human PBMCs (5×10^5 cells/well) and incubated with the indicated doses of antibodies. The spontaneous release samples were stained for target cells without effector cells, and the maximum release samples were stained for target cells with lysis solution. After 3 h of incubation at 37 °C in 5% CO2, the supernatant was harvested and transferred to new plates with excitation and emission wavelengths of 485 and 520 nm, respectively, via an FLx800™ Spectramax (Bio-Tek).

Mouse models

Six- to eight-week-old human 4-1BB knock-in C57BL/6 and BALB/C mice were purchased from Gempharmatech Co., Ltd. (JiangSu, China). The mice were housed under SPF conditions, acclimated for 7 days prior to use and kept on a 12/12-hour light/dark cycle with food and water provided ad libitum. Human 4-1BB knock-in C57BL/6 and BALB/C mice were subcutaneously injected with MC38/MSLN tumour cells (1×10^6/mouse) or CT26/MSLN tumour cells (2×10^6/mouse). When the tumour size reached ~ 50 mm^3 (MC38/MSLN) or ~ 75 mm^3 (CT26/MSLN), the tumour-bearing mice were randomly assigned to different study groups. Groups of five animals each were intravenously administered HK013-G1 or HK013-G4 at 1 or 6 mg/kg twice weekly for up to 3 weeks. The tumour volume was monitored twice per week. The tumour length and width were measured. The tumour volume was calculated according to the following equation: 0.5 × length × width × width. The mice were sacrificed once the tumour volume reached 3000 mm3. For the hepatotoxicity study, treated mice bearing MC38/MSLN tumours were euthanized, and serum was collected for AST/ALT detection. For the rechallenge experiment, 1.25×10^6 CT26 cells were implanted subcutaneously into the left flank of CT26/MSLN tumour model mice that achieved complete remission 30 days after the final vaccination.

In vitro cytokine release assay

PBMCs from healthy donors in RPMI-1640 medium supplemented with 10% FBS in 96-well flat-bottom plates (2×10^5 cells/well) were treated with 10–0.1 μg/ml of the tested antibodies for 48 h. The levels of the cytokines IFN-γ, TNF-α, IL-10, IL-2, IL-6, IL-4 and IL-17a in the culture medium were measured via a cytometric bead array assay (C60021, QuantoBio) according to the manufacturer's instructions. The fluorescence signals were measured via the CytoFlex system.

Pharmacokinetics and toxicity study

Single- and repeat-dose studies were performed. In the pharmacokinetic study, cynomolgus monkeys were intravenously injected with HK013-G1 at a single dose of 3 or 30 mg/kg (two males and two females in each group). Serum samples for drug concentration determination were collected from all animals before and after drug administration for 5 min and 2, 8, 24, 48, 72, 120, 168, 240 and 288 h. Serum HK013-G1 concentrations were measured via sandwich ELISA using human MSLN-His, human 4-1BB-mFc and HRP-conjugated goat anti-mouse Fc antibody (Jackson). For the 5-week repeated-dose toxicity study, cynomolgus monkeys were given HK013-G1 (3 or 30 mg/kg) once a week for five i.v. infusions. Each group consisted of two males and two females. Safety and toxicity were assessed on the basis of standard parameters.

These studies all have been approved by IACUC of University of Science and Technology of China as the proposal No. 2021-N(A)-083. We performed them in strict accordance with the guidelines established by the IACUC.

Statistical analysis

Statistical analysis was performed via GraphPad Prism 9 software (GraphPad Software, Inc.). Two-tailed t tests were used to compare the treatment groups with the control groups. A P value of < 0.05 was considered to indicate statistical significance.

Results

Characterization of the HK013 antibody

We designed an anti-MSLN×4-1BB bispecific antibody for the two subtypes to compare their antitumour effects (Fig. 1a). HK013-G1 was generated by fusing a single-chain variable fragment (scFv) of an anti-4-1BB antibody (HuB6, patent WO2021093753A1) at the C-terminus of the heavy chain of a humanized anti-MSLN IgG1 nanobody (R2G12, patent WO2019246003A1) in a symmetric manner. HK013-G4 was derived from HK013-G1 by replacing IgG1 with IgG4. HK013-G1/4 bound to both human MSLN and 4-1BB proteins with an EC50 of approximately 0.05 nM for the two antigens (Fig. 1b, Supplementary Fig. s1a-b), and the affinity of HK013-G1/4 for human MSLN was more than tenfold greater than that for human 4-1BB (Supplementary Table 1). Similarly, these compounds could react against cynomolgus monkey MSLN and 4-1BB (Supplementary Fig. s1c-d). Moreover, HK013-G1/G4 blocked CA125 binding to MSLN, as did the mouse-human chimeric IgG1 monoclonal antibody MORAb-009 (amatuximab), which implies that the antibodies should inhibit the adhesion and viability of cancer cells and increase chemosensitivity (Fig. 1c) [14, 16].

Next, we determined MSLN expression on the cell surface and selected high-, moderate- and low-MSLN-expressing NCI-H226, OVCAR3 and AsPC-1 cells as representative cancer cell lines for further study (Supplementary Table 2). As demonstrated by flow cytometry analysis, HK013-G1/G4 bound NCI-H226, OVCAR3 and AsPC-1 cells in a concentration-dependent manner, similar to the anti-MSLN IgG1 nanobody R2G12 (Fig. 1d). Moreover, we confirmed that HK013-G1/G4 could effectively link MSLN-expressing cells and 4-1BB-expressing cells together (Fig. 1e).

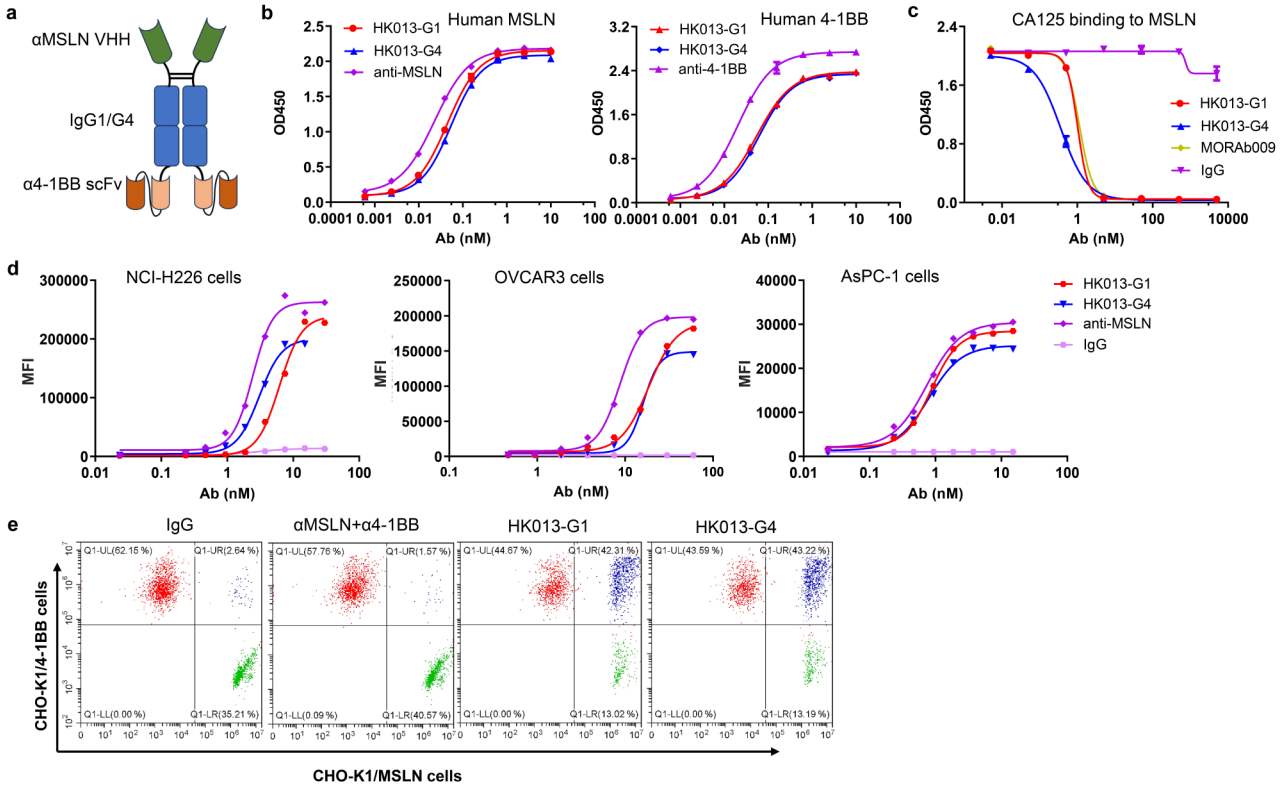

Fig. 1 Characterization of HK013-G1. (**a**) Structural overview of HK013-G1/G4. (**b**) The activities of HK013-G1/G4 against human MSLN and 4-1BB proteins were detected via ELISA. Anti-MSLN R2G12 and anti-4-1BB HuB6 were both used as positive controls. (**c**) The blockage of CA125 binding to the MSLN protein by HK013-G1/G4 was measured via ELISA. MORAb-009 (MORAb) was used as a positive control. (**d**) The binding activities of HK013-G1/G4 to MSLN-expressing cancer cell lines were evaluated via flow cytometry. MFI: mean fluorescence intensity. NCI-H226, OVCAR3 and AsPC-1 cells presented high, moderate and low MSLN expression, respectively. The anti-MSLN IgG1 nanobody R2G12 was used as a positive control. (**e**) The capacity of HK013-G1/G4 cells to bridge MSLN-expressing and 4-1BB-expressing cells was evaluated via flow cytometry. The results are representative of three independent experiments. *, $P < 0.05$; **, $P < 0.01$; ***, $P < 0.001$

HK013-G1/G4 activates 4-1BB signaling in a manner dependent on MSLN engagement

One of the biomarkers of 4-1BB signaling activation in cytotoxic T cells is increased production of IFN-γ [9, 17]. Therefore, we first assessed CD8 + T-cell activation induced by HK013-G1/G4. As expected, HK013-G1/G4 induced potent IFN-γ secretion, even more than urelumab did when the concentration was not above 1 nM ($P < 0.05$). Furthermore, HK013-G1/G4 activated CD8 + T cells to secrete IFN-γ only when they were cocultured with MSLN-positive cells. However, urelumab still increased IFN-γ secretion when the concentration was not less than 1 nM (Fig. 2a). To further investigate whether the 4-1BB signaling activity of HK013 is strictly dependent on MSLN engagement, we constructed a detection system in which the luciferase reporter HEK-293/NFκB-Luci/4-1BB cells were cocultured with different MSLN-expressing MC38 cells, including MC38/MSLN^{hi}, MC38/MSLN^{mid} and MC38/MSLN^{low} cells. Consistent with the previous results, HK013-G1/G4 induced stronger 4-1BB signaling than urelumab did in MC38/MSLN^{mid} ($P < 0.05$) and MC38/MSLN^{hi} cells ($P < 0.001$). In MC38/MSLN^{low} cells, HK013-G1/G4 did not exhibit obvious activity when the HK013-G1/G4 concentration was not greater than 1 nM. However, urelumab had a similar effect on all the MC38/MSLN cells (Fig. 2b). These results demonstrated that HK013-mediated activation of 4-1BB signaling is strictly dependent on MSLN expression in the tumour environment.

Moreover, our results revealed that HK013-G1 and HK013-G4 had similar effects on 4-1BB signaling activation (Fig. 2a,b). However, they did not show the same activation profiles of 4-1BB signaling when the treated CHO-K1 cells expressed different FcγRs (FcγRI, FcγRIIA or FcγRIIB). HK013-G1 showed stronger activity than HK013-G4 did when the concentration was not less than

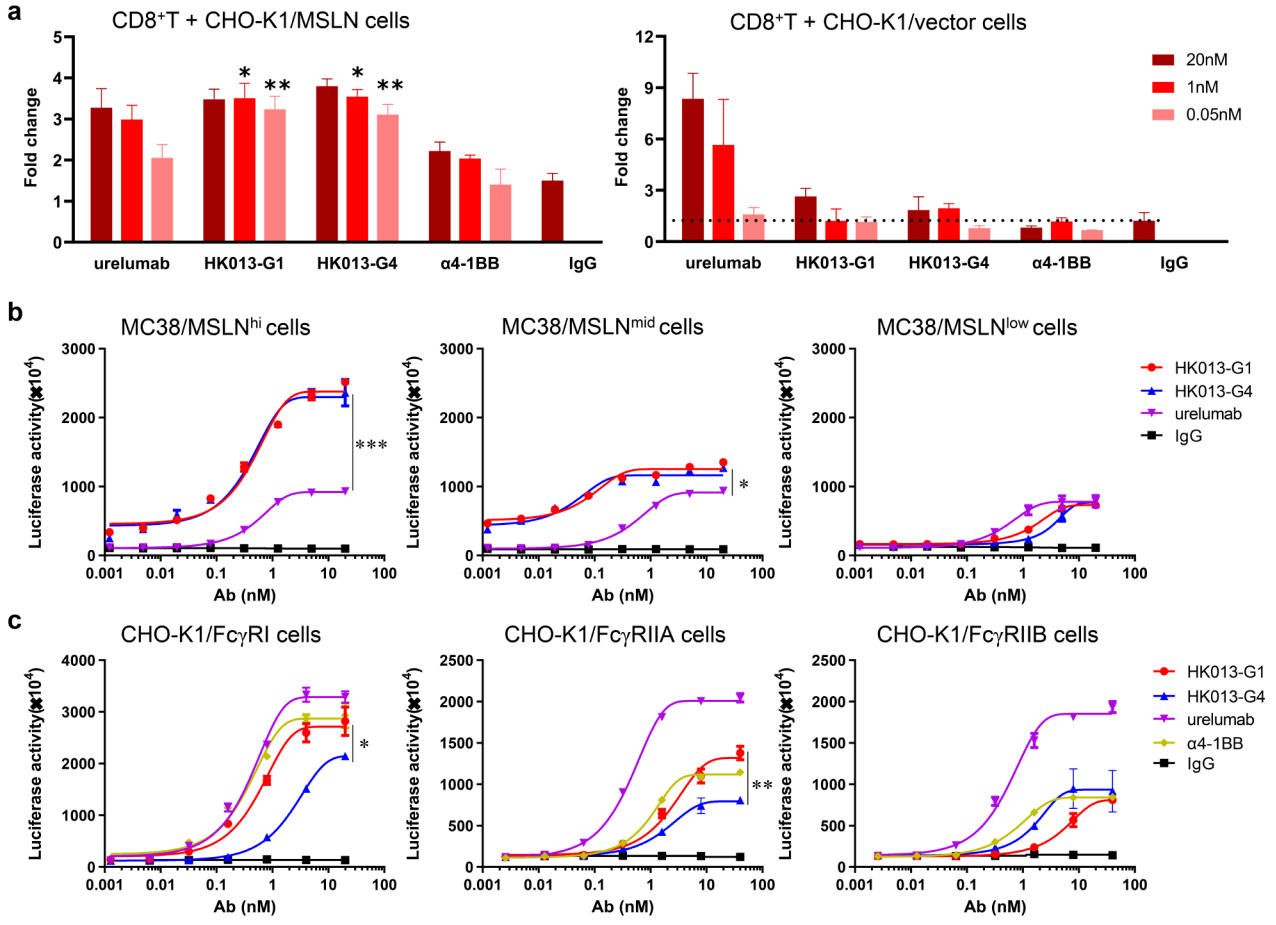

Fig. 2 Immune activation ability of HK013-G1. (**a**) CD8 + T cells cocultured with MSLN-expressing cells were treated with the indicated antibodies for 4 days. The IFN-γ concentration in the medium was measured via ELISA. CHO-K1/vector cells were used as a negative control. Compared with urelumab, *, $P < 0.05$; **, $P < 0.01$. **(b)** Luciferase activity was determined in HEK-293/NFκB-Luci/4-1BB cells cocultured with different MSLN-expressing MC38/MSLN cells after treatment with the indicated antibodies for 14 h. *, $P < 0.05$; ***, $P < 0.001$. (**c**) Luciferase activity was determined in HEK-293/NFκB-Luci/4-1BB cells cocultured with different FcγR-engineered CHO-K1 cells after treatment with the indicated antibodies for 14 h. All the experiments were performed three times independently. *, $P < 0.05$; **, $P < 0.01$

0.1 nM, the FcγR was FcγRI ($P<0.05$), the concentration was not less than 10 nM, and the FcγR was FcγRIIA ($P<0.01$). However, they presented a similar activity curve in the presence of FcγRIIB (Fig. 2c). Our results indicated that the Fc subtype of HK013 should not significantly affect 4-1BB signaling activity except under certain specific conditions, such as FcγRI and FcγRIIA.

HK013-G1 effectively kills tumour cells in vitro

HK013-G1 was designed to retain the Fc effector function through the adoption of the IgG1 Fc region. The ADCC reporter assay using the FcγRIIIa Jurkat effector HK013-G1 induced an obvious ADCC effect in MSLN-positive OVCAR3 cells in a dose-dependent manner, which was superior to that of the positive control MORAb-009. However, HK013-G4 had no significant effect (Fig. 3a). Furthermore, HK013-G1 induced more marked effects than HK013-G4 did on the induced cytotoxicity of human PBMCs and NK cell activity ($P<0.01$, Fig. 2b,c). Therefore, HK013-G1 was selected for further examination. As expected, HK013-G1 efficiently directed NK92 cells to lyse MSLN-positive tumour cells, including high-expressing NCI-H226, moderate-expressing OVCAR3 and low-expressing AsPC-1 cells. However, no effect was observed in MSLN-negative HEK293 cells, which indicated that HK013-G1 should have strict specificity for MSLN expression (Fig. 3d). Moreover, the IFN-γ release and NF-κB luciferase activity of HK013-G1 cells did not significantly change in the presence of soluble MSLN (sMSLN) (Fig. 3e). In addition, HK013-G1 had no obvious complement-dependent cytotoxicity (CDC) effect on MSLN-positive tumour cells (Supplementary Fig. s2).

HK013-G1 induces potent antitumour immunity in vivo

The in vivo antitumour activity of HK013-G1 was evaluated in human 4-1BB knock-in mice bearing MSLN-positive tumours. In the MC38/MSLN model, HK013-G1 treatment had significant tumour-inhibitory efficacy at a dose of 1 mg/kg compared with the PBS control ($P<0.05$) and had a greater effect at the 6 mg/kg dose ($P<0.01$). However, HK013-G4 had no significant effect at a dose of 1 mg/kg and had a tumour-inhibitory effect at a dose of 6 mg/kg (Fig. 4a). Specifically, HK013-G1 exhibited superior antitumour efficacy, with an 89% tumour growth inhibition (TGI) rate at 6 mg/kg compared with the same dose of HK013-G4, with a 70% TGI rate, which was near the 63% TGI rate of 1 mg/kg HK013-G1 (Fig. 4b). In the

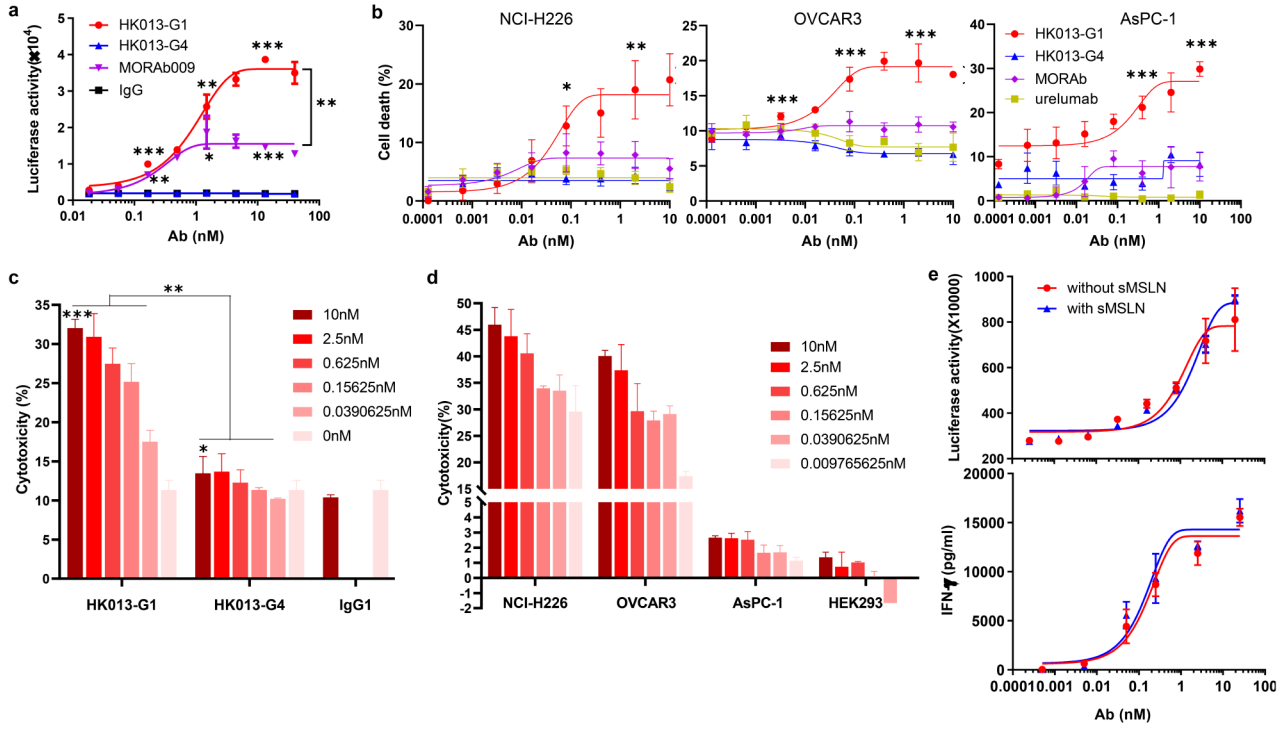

Fig. 3 Antitumour effects of HK013-G1 in vitro. (**a**) ADCC activity was detected after the indicated antibody treatment for 18 h. FcγRIIIa Jurkat effector and target OVCAR3 cells were cocultured at E: T = 1:1. (**b**) The cytotoxicity was measured via the calcein retention method. Calcein-AM-labeled OVCAR3 cells were incubated with human PBMCs at an E: T ratio of 50:1 and treated with the serially diluted indicated antibody for 3 h. (**c**) The activity of HK013 NK cells was analyzed via an LDH assay. NK92 and target OVCAR3 cells were cocultured at an E: T ratio of 5:1 and treated with serially diluted HK013-G1/G4 for 3.5 h. (**d**) The activity of HK013-G1 NK cells was measured via LDH assay. NK92 and NCI-H226, OVCAR3, AsPC-1 or HEK293 cells were cocultured at E: T = 5:1 and treated with serially diluted HK013-G1 for 3.5 h. (**e**) The reporter luciferase activity and IFN-γ release induced by HK013-G1 did not significantly change in the presence of 0.5 μg/mL soluble MSLN (sMSLN). All the experiments were performed three times independently. *, $P<0.05$; **, $P<0.01$; ***, $P<0.001$

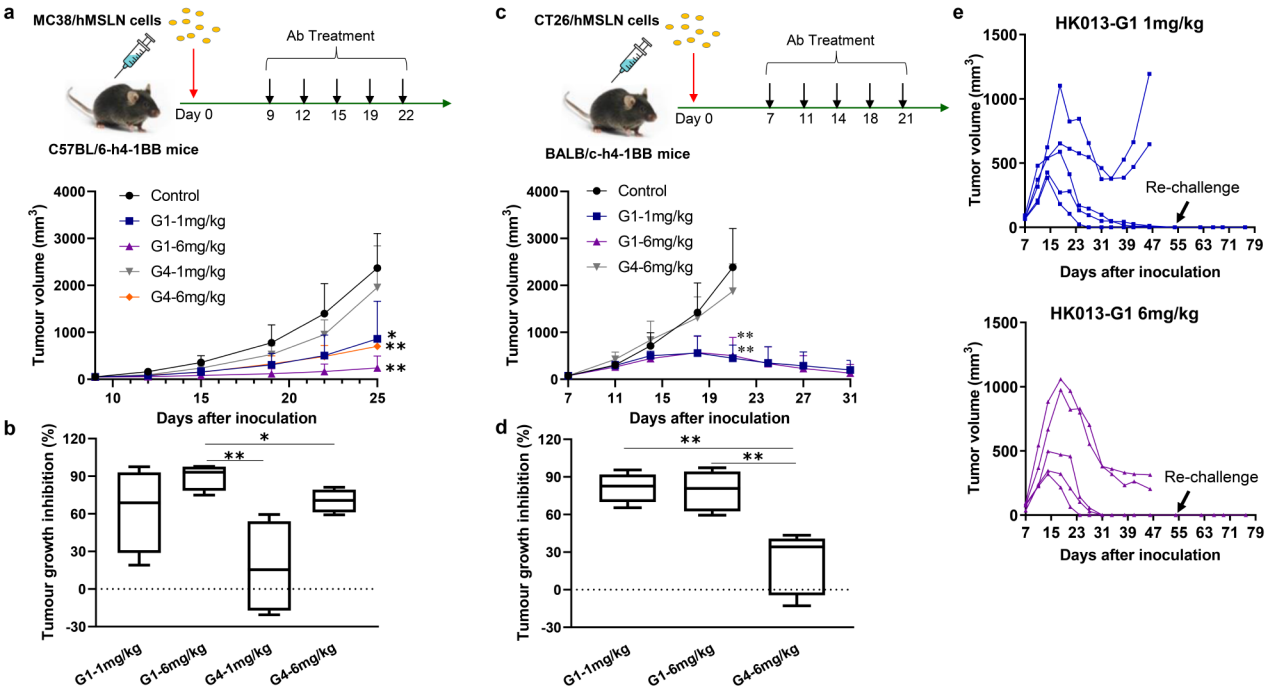

Fig. 4 Antitumour efficacy of HK013-G1 in humanized mouse models. (**a**) Human 4-1BB-KI C57BL/6 mice bearing MC38/MSLN tumours were treated with HK013-G1/G4 (1 or 6 mg/kg) five times ($n=5$). The tumour volume was monitored twice per week. (**b**) Tumour growth inhibition (TGI) analysis for (**a**). (**c**) Human 4-1BB-KI C57BL/6 mice bearing CT26/MSLN tumours were treated with HK013-G1 (1 or 6 mg/kg) or HK013-G4 (6 mg/kg) five times ($n=5$). Tumour growth was measured twice per week. (**d**) Three mice in (B) with complete remission were rechallenged with 1.25×10^6 CT26 cells 30 days after HK013-G1 treatment. *, $P<0.05$; **, $P<0.01$

CT26/MSLN model, HK013-G1 reduced the tumour volume in both the 1 mg/kg and the 6 mg/kg groups compared with the control ($P<0.01$). However, HK013-G4 did not markedly inhibit tumour growth even at a dose of 6 mg/kg (Fig. 4c). For TGI, HK013-G1 had rates of 78% and 81% at 1 mg/kg and 6 mg/kg, respectively, and 6 mg/kg HK013-G4 had a 21% rate (Fig. 4d). Notably, three out of the five mice in the two HK013-G1-treated groups exhibited complete tumour regression, and all the cured mice were protected against CT26/MSLN tumour rechallenge. Although three CT26/MSLN tumours also disappeared in the 1 mg/kg HK013-G1 group, the 6 mg/kg HK013-G1 group presented complete tumour regression on d31, which occurred 16 days earlier than the 1 mg/kg HK013-G1 group did (Fig. 4e).

HK013-G1 has high safety

To examine the possible nonspecific cytokine release induced by HK013-G1, human PBMCs were incubated with the tested antibodies for 2 days. Compared with the IgG control, HK013-G1 did not increase the release of inflammatory cytokines, including TNFα, IL-10, IL-17α, IL-6, IL-2, IFNγ and IL-4, similar to anti-4-1BB HuB6 (Fig. 5a, Supplementary Fig. s3).

Since HK013-G1 reacts to MSLN and 4-1BB in cynomolgus monkeys (Supplementary Fig. s1c-d), in vivo pharmacokinetic (PK) and toxicokinetic (TK) studies were performed on cynomolgus monkeys intravenously injected with 3 or 30 mg/kg HK013-G1. The mean half-lives of HK013-G1 were approximately 61 h (2.5 days) and 97 h (4 days) at single doses of 3 and 30 mg/kg, respectively (Fig. 5b).

In the weekly 3 mg/kg dose study, the serum IL-6 level increased at 2 h after the first HK013-G1 injection and gradually decreased to the control level or baseline level on the next day. However, the IL-2 levels remained stable at 43 days. In the repeated 30 mg/kg dose study, the IL-6 level slightly increased, and the IL-2 content first increased but then decreased (Fig. 5c). Moreover, the proportion of T lymphocytes did not significantly change, except that the ratios of CD45 + CD3 + T and CD45 + CD3 + CD4 + T cells mildly decreased in the female monkeys treated with the 30 mg/kg dose. The proportion of CD3-CD16 + NK cells slightly increased, except that the 3 mg/kg dose did not markedly change after HK013-G1 treatment (Fig. 5d). No obvious adverse symptoms occurred in the treated cynomolgus monkeys.

In addition, toxicity evaluation was also performed in human 4-1BB-KI C57B6 mice bearing MC38/MSLN tumours by intravenous injection of 10 mg/kg repeated-dose antibodies (Supplementary Fig. s3a). HK013-G1 and HK013-G4 did not induce significant side effects,

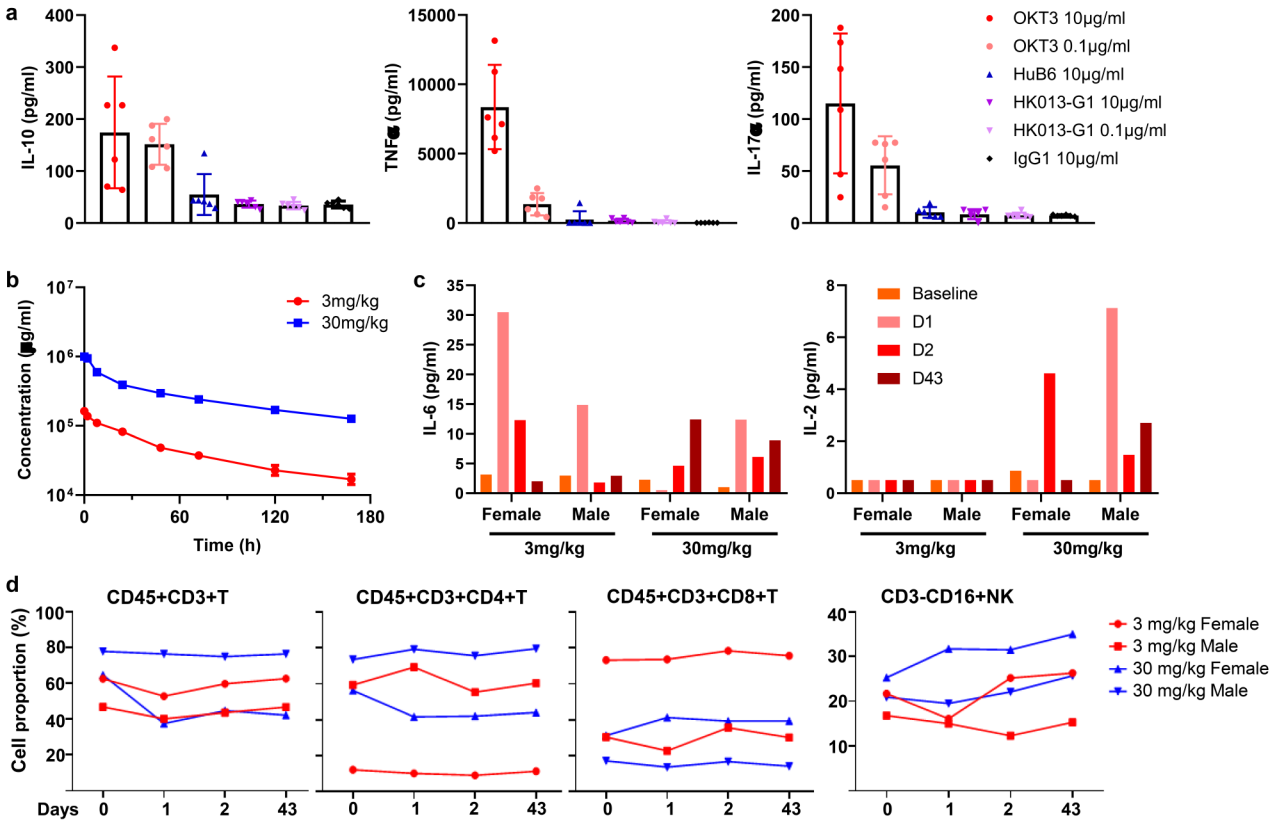

Fig. 5 Safety profile of HK013-G1. (**a**) PBMCs were incubated with 10–0.1 μg/ml of the tested antibodies for 48 h. The released cytokine level in the culture medium was measured. (**b**) HK013-G1 serum concentrations were measured after a single intravenous injection of 3 or 30 mg/kg HK013 into cynomolgus monkeys. HK013-G1 concentrations were measured via sandwich ELISA using human MSLN-His and human 4-1BB-mFc. (**c**) Transient CD45 + CD3 + T, CD45 + CD3 + CD4 + T, CD45 + CD3 + CD8 + T and CD3-CD16 + NK lymphocyte proportions were measured via flow cytometry in the blood before, 2 h after the first dose (D1), 24 h after the first dose (D2) and during the recovery phase (D43). (**d**) Serum IL6 and IL-2 cytokine release in cynomolgus monkeys at predose, 2 h after the first dose (D1), 24 h after the first dose (D2) and during the recovery phase (D43). LLOQ, lower limit of quantitation

whereas two mice in the urelumab group presented elevated serum AST and ALT levels and obvious immune cell infiltration into the liver (Supplementary Fig. s3b-c). Overall, HK013-G1 was well tolerated by mice and cynomolgus monkeys.

Discussion

Agonists against 4-1BB and other TNFRSF members require effective crosslinking to induce receptor oligomerization, which generally employs FcγR engagement [18–20]. However, owing to the wide distribution of Fc receptors, ensuring the safety of one antibody drug with an intact Fc is a great challenge [21]. Moreover, most 4-1BB agonists are inclined to induce global immune activation and result in systemic toxicity; thus, a BsAb drug design is favored for 4-1BB activation, which is dependent on TAA expression [22–24]. In this study, we generated an optimized targeting agonist, HK013-G1, by fusing the anti-4-1BB scFv to the C-terminus of the anti-MSLN VHH, which contains a human IgG1 Fc domain. HK013-G1 was confirmed to stimulate 4-1BB signaling in a manner dependent on the MSLN protein and effectively killed MSLN-positive cancer cells without systemic immune activation or associated hepatotoxicity.

The optimization strategies of HK013-G1 include three main points. First, molecules with smaller molecular weight are more likely to enter the tumour microenvironment, which is favorable for cancer immunotherapy [25, 26]. The use of anti-MSLN VHH and anti-41BB scFv can reduce the overall molecular weight of HK013-G1 to ~ 130 kDa, which is close to that of monoclonal antibodies. We speculate that this phenomenon is conducive to the diffusion of HK013-G1 into tumour tissues. Thus, it can bind better to T cells and exert antitumour activity. Moreover, the anti-MSLN VHH could block the interaction of CA125 with MSLN and prevent the proliferation and migration of tumour cells [16, 27]. Second, by adopting a scFv targeting 4-1BB at the C-terminus of the Fc domain, HK013-G1 could bridge MSLN- and 4-1BB-expressing cells and mediate 4-1BB signaling activation in a manner strictly dependent on MSLN, similar to the reported BsAb M9657 [28]. Third, the affinity of

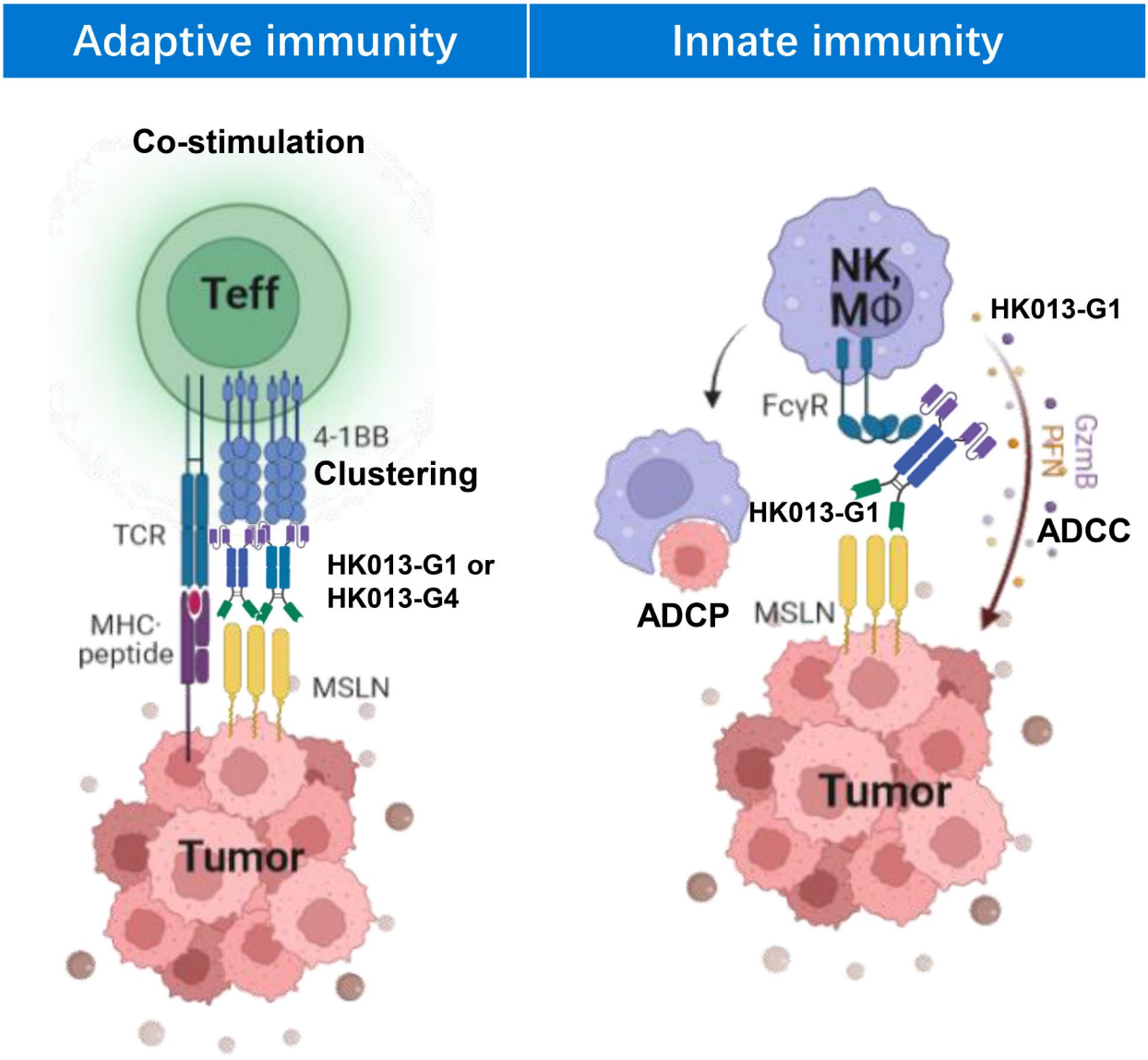

Fig. 6 Schematic illustration of the mechanism of action of HK013-G1. On the one hand, HK013 mediates the induction of adaptive immunity by stimulating 4-1BB signaling in T cells by simultaneously binding to MSLN expressed on tumour cells and 4-1BB expressed on T lymphocytes, resulting in the clustering of 4-1BB molecules. On the other hand, HK013-G1 functions in ADCC through the interaction of its Fc with the FcR on the surface of innate immune cells, thereby inducing an innate immune response. The antitumour effect of HK013-G1 depends on both innate and adaptive immunity

HK013-G1 for MSLN was designed to be greater than that for 4-1BB to ensure the specific targeting of MSLN-positive cells and reduce possible toxicity. This design was tested successfully in our previous BsAb HK010 [11].

The antitumour effect of HK013-G1 should depend on both innate and adaptive immunity. As so far, most BsAbs that target immunostimulatory receptors employ IgG4 weakly bound to Fc receptors or IgG1 with silent mutations; thus, they lack Fc-related functions, including ADCC and CDC [29–31]. However, the ADCC effect is very favorable for TAA targets in cancer immunotherapy [32–34]. Therefore, we retained the ADCC function of HK013-G1 by adopting a human IgG1 subtype. HK013-G1 has an ADCC effect through the interaction of its Fc with the FcR on the surface of innate immune cells, thereby inducing an innate immune response (Fig. 6). As shown in Fig. 3a,b, HK013-G1 even had a stronger ADCC effect than did MORAb-009/amatuximab with human IgG1. However, HK013-G4 did not have this effect. Therefore, HK013-G1 induced lysis of MSLN-positive tumour cells when cocultured with human PBMCs, but HK013-G4 did not. On the other hand,, HK013-G1 mediated the induction of adaptive immunity by stimulating the 4-1BB signaling pathway by simultaneously binding

to MSLN expressed on tumour cells and 4-1BB expressed on T lymphocytes, resulting in the clustering of 4-1BB molecules. Importantly, target cell lysis and T-cell activation by HK013-G1 were dependent on MSLN expression in cancer cells with the high specificity, as these effects were not observed in cancer cells lacking MSLN expression. In addition, previous studies have shown that the shedding of soluble MSLN into tumours impairs the efficacy of MSLN-targeted therapy [35, 36]. Although HK013-G1 possibly binds to soluble MSLN, it has no significant effect on HK013-G1-induced T-cell activation in vivo. Thus, the effect of soluble MSLN on the clinical benefit of the drug would be greatly reduced. In addition, in the Fc receptor-mediated 4-1BB signal activation reporter assay, HK013-G1 had much lower activity than urelumab and was comparable to 4-1BB and HK013-G4. Therefore, the selection of the IgG1 subtype for HK013-G1 does not increase the risk of hepatotoxicity associated with Fc receptor occupancy. Moreover, our in vivo study revealed that the antitumour efficacy of HK013-G1 was superior to that of HK013-G4, which indicated that the superiority of HK013-G1 is dependent mainly on the function of IgG1 Fc. In addition, HK013-G1 remained effective even in the presence of sMSLN, similar to the effects of the BsAb MSLN490 [15]. The high biological activity, safety, and favorable pharmacokinetic properties of HK013-G1 support studies testing its clinical activity in patients with MSLN-expressing cancers.

At present, a variety of MSLN-targeted therapies have been clinically applied to MSLN-positive solid tumours, including mesothelioma, pancreatic cancer, ovarian cancer, and lung adenocarcinoma [37, 38], and some clinical benefits have been shown, especially in ovarian cancer [39]. The antitumour effects of HK013-G1 observed in vitro and in mouse tumour models suggest that HK013-G1 may play a therapeutic role in MSLN-positive solid tumours. Additionally, Single-dose PK analysis revealed that the mean half-lives of HK013-G1 were approximately 61 h (2.5 days) and 97 h (4 days) at 3 and 30 mg/kg, respectively, which are within normal limits considering that HK013-G1 is composed of a nanobody [40, 41]. PK data from cynomolgus monkeys suggest that a weekly dosing schedule may be sufficient to maintain an appropriate plasma drug concentration of HK013-G1 to exert clinical antitumour activity.

In the cynomolgus monkeys, none of the tested doses led to changes in the lymphocyte proportion, and only the 30 mg/kg HK013-G1 led to an increase of IL-6 release. As IL-6 is a central mediator of cytokine responses in cytokine release syndrome (CRS), this phenomenon may imply that high doses of HK013-G1 are associated with a risk of causing CRS, an adverse event that has been observed in MSLN-CAR-T-cell therapy [42]. Therefore, the levels of IL-6 and other CRS-related cytokines, such as IFNγ and IL-2, should be closely monitored in clinical trials. On the other hand, anti-IL-6 receptor antagonists or corticosteroids, which are usually effective in the management of treatment-mediated CRS in TCE or CAR-T-cell clinical trials [43, 44], could be considered for use with HK013-G1.

Molecules bridging CD3ε on T cells with MSLN on cancer cells have entered the clinic, but owing to the risk of CRS [43], the clinical dose of these drugs is low, just as the dose of CD3-based TCEs in NHPs is mostly at the microgram level; thus, it is difficult to obtain better clinical benefits in solid tumours. However, bispecific antibody based on costimulatory molecules, such as the anti-CD40xMSLN molecule, are relatively safe; unfortunately, its clinical benefit is poor [45, 46]. Therefore, we developed HK013-G1 cells with both adaptive and innate immunity. Despite changes in IL-6 release, HK013-G1 was remarkably well tolerated up to 30 mg/kg after repeated administration without gross macroscopic findings or dose-limiting toxicity. Notably, the Cmax at the 30 mg/kg dose was approximately 1 mg/kg (~7.75 μM), which exceeded the maximum value in vitro for T-cell activation and target cell lysis. The pharmacodynamics and toxicology evaluation of HK013-G1 in NHPs suggest the potential for a wide therapeutic window.

As a costimulatory molecule, 4-1BB can coordinate with CD3 to promote T-cell proliferation and activation [47]. In fact, 4-1BB agonist antibodies have been shown to enhance tumour-infiltrating T-cell expansion and antitumour activity in combination with CD3-based antibodies [48]. Additionally, tumour-infiltrating T cells frequently coexpressed 4-1BB and PD-1 receptors in a mouse tumour model, and the combination of PD-(L)1 inhibition and 4-1BB agonists had synergistic antitumour effects [49, 50]. Moreover, many clinical trials of anti-4-1BB in conjunction with anti-PD-(L)1 or anti-4-1BB/PD-(L)1 bispecific antibodies are currently underway [5]. Similarly, clinical benefits from MSLN CAR-T cells combined with anti-PD1 antibodies have also been observed in patients with mesothelioma [51, 52]. Hence, combining HK013-G1 with CD3-based TCE or PD-(L)1 inhibitors may be a useful strategy for improving clinical benefits.

Conclusions

Together, we presented a novel humanized anti-MSLN×4-1BB BsAb, HK013-G1, with an IgG1 Fc. HK013-G1 exhibited a potent antitumour effect only in the MSLN-positive tumour microenvironment through the induction of both innate and adaptive immunity. In particular, HK013-G1 did not induce nonspecific production of proinflammatory cytokines or obvious liver toxicity. Our studies demonstrate that overcoming the challenges that have hampered the clinical development

of MSLN-targeted drugs for solid tumours may be possible. These results suggest that HK013-G1 has potent antitumour activity and a safe safety profile and support the clinical development of HK013-G1 in patients with MSLN-positive tumours for whom better treatment options are needed.

Supplementary Information

The online version contains supplementary material available at https://doi.org/10.1186/s12967-025-06107-z.

Supplementary Material 1

Author contributions

LC, GS and YH were responsible for the study design and supervision. DZ, ZZ and AS were responsible for the study implementation and writing of the manuscript. WL, WZ and PZ were responsible for the data analysis and interpretation. JW, XD and XZ were responsible for the model animal experiments. YZ, HL and HZ were responsible for the expression, purification and quality control of the antibodies. All the authors participated in drafting the manuscript and approved the final version of the manuscript.

Funding

This work was supported by the Joint Research Center for Biomedicine of IHM (2023HAK0013), Anhui Provincial Natural Science Foundation (2408085QH250), Joint Fund for Synchrotron Radiation at USTC (KY9110000001) and USTC Research Funds of the Double First-Class Initiative (YD9110002069).

Data availability

This article includes the datasets that support our findings.

Declarations

Ethics approval and consent to participate

This study was conducted with the approval of the Ethics Committee of the Shanghai Zhaxin Hospital of Integrated Traditional Chinese & Western Medicine and in accordance with the guidelines for Good Clinical Practice and the Declaration of Helsinki. All animal experiments were approved by the Ethics Committee for Animal Experiments of The First Affiliated Hospital of the University of Science and Technology of China [2021-N(A)-083] and performed in accordance with the guidelines for animal experiments in laboratories. Endpoints such as euthanasia were considered appropriate if the animals experienced intolerable pain (such as gait disturbance, water/feeding impairment, a tumour diameter of 20 mm or more, a tumour volume of 4000 mm^3 or more, or 25% or more weight loss in 7 days).

Consent for publication

Not applicable.

Competing interests

The authors declare that they have no competing interests.

Author details

[1]Department of Medical Oncology, Division of Life Sciences and Medicine, The First Affiliated Hospital of USTC, University of Science and Technology of China, Anhui Provincial Cancer Hospital, Hefei 230031, Anhui, China
[2] Hefei HankeMab Biotechnology Co., Ltd.; Anhui Province Key Laboratory of Gene Engineering Pharmaceutical, Biomedicine Technology Innovation Center of Hefei, Anhui Anke Biotechnology (Group) Co., Ltd, Hefei 230031, Anhui, China
[3]Anhui Province Key Laboratory of Geriatric Immunotherapy and Nutrition Therapy, Gerontology Institute of Anhui Province, Hefei 230001, Anhui, China
[4]Department of General Surgery, Division of Life Sciences and Medicine, The First Affiliated Hospital of USTC, University of Science and Technology of China, Hefei 230001, Anhui, China
[5]Department of Geriatrics, Division of Life Sciences and Medicine, The First Affiliated Hospital of USTC, University of Science and Technology of China, Hefei 230001, Anhui, China

Received: 1 September 2024 / Accepted: 8 January 2025
Published online: 13 January 2025

References

1. Doroshow DB, et al. PD-L1 as a biomarker of response to immune-checkpoint inhibitors. Nat Rev Clin Oncol. 2021;18(6):345–62.
2. Bai Y, et al. Efficacy and predictive biomarkers of immunotherapy in Epstein-Barr virus-associated gastric cancer. J Immunother Cancer. 2022;10(3):e004080.
3. Olson DJ, et al. Pembrolizumab Plus Ipilimumab following Anti-PD-1/L1 failure in Melanoma. J Clin Oncol. 2021;39(24):2647–55.
4. Pichler AC, et al. TCR-independent CD137 (4-1BB) signaling promotes CD8+-exhausted T cell proliferation and terminal differentiation. Immunity. 2023;56(7):1631–e4810.
5. Melero I, et al. CD137 (4-1BB)-Based Cancer Immunotherapy on its 25th anniversary. Cancer Discov. 2023;13(3):552–69.
6. Palmeri JR, et al. CD8 + T cell priming that is required for curative intratumorally anchored anti-4-1BB immunotherapy is constrained by Tregs. Nat Commun. 2024;15(1):1900.
7. Segal NH, et al. Results from an Integrated Safety Analysis of Urelumab, an agonist Anti-CD137 monoclonal antibody. Clin Cancer Res. 2017;23(8):1929–36.
8. Segal NH, et al. Phase I study of single-Agent Utomilumab (PF-05082566), a 4-1BB/CD137 agonist, in patients with Advanced Cancer. Clin Cancer Res. 2018;24(8):1816–23.
9. Cheng LS, et al. A humanized 4-1BB-targeting agonistic antibody exerts potent antitumor activity in colorectal cancer without systemic toxicity. J Transl Med. 2022;20(1):415.
10. Hinner MJ, et al. Tumor-localized Costimulatory T-Cell Engagement by the 4-1BB/HER2 bispecific antibody-Anticalin Fusion PRS-343. Clin Cancer Res. 2019;25(19):5878–89.
11. Cheng LS, et al. An Fc-muted bispecific antibody targeting PD-L1 and 4-1BB induces antitumor immune activity in colorectal cancer without systemic toxicity. Cell Mol Biol Lett. 2023;28(1):47.
12. Gao J, et al. CLDN18.2 and 4-1BB bispecific antibody givastomig exerts antitumor activity through CLDN18.2-expressing tumor-directed T-cell activation. J Immunother Cancer. 2023;11(6):e006704.
13. Hassan R, et al. Mesothelin-targeting T cell receptor fusion construct cell therapy in refractory solid tumors: phase 1/2 trial interim results. Nat Med. 2023;29(8):2099–109.
14. Matsuzawa F, et al. Mesothelin blockage by Amatuximab suppresses cell invasiveness, enhances gemcitabine sensitivity and regulates cancer cell stemness in mesothelin-positive pancreatic cancer cells. BMC Cancer. 2021;21(1):200.
15. Liu JJ et al. T cell-redirecting antibody for treatment of solid tumors via targeting mesothelin. Acta Pharmacol Sin. 2024 Jun 10.
16. Rupert PB, et al. Structural elucidation of the mesothelin-mucin-16/CA125 interaction. Structure. 2024;32(8):1049–e542.
17. Wang H, et al. CD137 ligand feedback upregulates PD-L1 expression on lung cancer via T cell production of IFN-γ. Thorac Cancer. 2019;10(12):2225–35.
18. Vanamee ÉS, Faustman DL. Structural principles of tumor necrosis factor superfamily signaling. Sci Signal. 2018;11(511):eaao4910.
19. Claus C et al. The emerging landscape of novel 4-1BB (CD137) agonistic drugs for cancer immunotherapy. MAbs. 2023 Jan-Dec;15(1):2167189.
20. Hangiu O, et al. Tumor targeted 4-1BB agonist antibody-albumin fusions with high affinity to FcRn induce anti-tumor immunity without toxicity. iScience. 2022;25(9):104958.
21. Bartkowiak T, et al. Activation of 4-1BB on Liver myeloid cells triggers Hepatitis via an Interleukin-27-Dependent pathway. Clin Cancer Res. 2018;24(5):1138–51.
22. Navarro R, et al. Pharmacokinetics and safety of LEAD-452, an EGFR-specific 4-1BB-agonistic trimerbody in non-human primates. Toxicol Appl Pharmacol. 2024;487:116961.

23. Jeong S, et al. Novel anti-4-1BB×PD-L1 bispecific antibody augments anti-tumor immunity through tumor-directed T-cell activation and checkpoint blockade. J Immunother Cancer. 2021;9(7):e002428.
24. Jeon SH et al. Anti-4-1BB×PD-L1 bispecific antibody reinvigorates tumor-specific exhausted CD8 + T cells and enhances the efficacy of Anti-PD-1 blockade. Clin Cancer Res. 2024 May 14.
25. Narbona J, et al. Nanobody-based EGFR-Targeting immunotoxins for Colorectal Cancer Treatment. Biomolecules. 2023;13(7):1042.
26. Verhaar ER, et al. Nanobodies in cancer. Semin Immunol. 2021;52:101425.
27. Li Q, et al. Preclinical evaluation of a novel anti-mesothelin immunotoxin based on a single domain antibody as the targeting ligand. Int J Pharm. 2021;602:120647.
28. Xu C, et al. M9657 is a bispecific tumor-targeted Anti-CD137 agonist that induces MSLN-Dependent Antitumor immunity without liver inflammation. Cancer Immunol Res. 2024;12(2):195–213.
29. Bannerji R, et al. Odronextamab, a human CD20×CD3 bispecific antibody in patients with CD20-positive B-cell malignancies (ELM-1): results from the relapsed or refractory non-hodgkin lymphoma cohort in a single-arm, multicentre, phase 1 trial. Lancet Haematol. 2022;9(5):e327–39.
30. Chu W, et al. HER2/PD1 bispecific antibody in IgG4 subclass with superior anti-tumour activities. Clin Transl Med. 2022;12(4):e791.
31. Engelberts PJ, et al. DuoBody-CD3xCD20 induces potent T-cell-mediated killing of malignant B cells in preclinical models and provides opportunities for subcutaneous dosing. EBioMedicine. 2020;52:102625.
32. Schram AM, et al. Zenocutuzumab, a HER2xHER3 bispecific antibody, is effective therapy for tumors driven by NRG1 gene rearrangements. Cancer Discov. 2022;12(5):1233–47.
33. Weisser NE, et al. An anti-HER2 biparatopic antibody that induces unique HER2 clustering and complement-dependent cytotoxicity. Nat Commun. 2023;14(1):1394.
34. Li HY, et al. Bispecific antibody targeting both B7-H3 and PD-L1 exhibits superior antitumor activities. Acta Pharmacol Sin. 2023;44(11):2322–30.
35. Awuah P, et al. Reduced shedding of Surface Mesothelin improves efficacy of mesothelin-targeting recombinant immunotoxins. Mol Cancer Ther. 2016;15(7):1648–55.
36. Snell D, et al. An engineered T-cell engager with selectivity for high mesothelin-expressing cells and activity in the presence of soluble mesothelin. Oncoimmunology. 2023;12(1):2233401.
37. Faust JR et al. Mesothelin: an immunotherapeutic target beyond solid tumors. Cancers (Basel), 2022. 14(6).
38. Chu Q. Targeting Mesothelin in Solid Tumours: anti-mesothelin antibody and drug conjugates. Curr Oncol Rep. 2023;25(4):309–23.
39. Mauricio D, et al. Novel mesothelin antibody-drug conjugates: current evidence and future role in the treatment of ovarian cancer. Expert Opin Biol Ther. 2021;21(8):1087–96.
40. Xenaki KT, et al. Homogeneous tumor targeting with a single dose of HER2-targeted albumin-binding domain-fused nanobody-drug conjugates results in long-lasting tumor remission in mice. Theranostics. 2021;11(11):5525–38.
41. Fleming BD, et al. Engineered Anti-GPC3 Immunotoxin, HN3-ABD-T20, produces regression in Mouse Liver Cancer xenografts through prolonged serum Retention. Hepatology. 2020;71(5):1696–711.
42. Tanyi JL, et al. Possible compartmental cytokine release syndrome in a patient with recurrent ovarian Cancer after treatment with mesothelin-targeted CAR-T cells. J Immunother. 2017;40(3):104–7.
43. Frey NV, Porter DL. Cytokine release syndrome with novel therapeutics for acute lymphoblastic leukemia. Hematol Am Soc Hematol Educ Program. 2016;2016(1):567–72.
44. Caimi PF, et al. Prophylactic Tocilizumab Prior to Anti-CD19 CAR-T cell therapy for Non-hodgkin Lymphoma. Front Immunol. 2021;12:745320.
45. Ye S, et al. A Bispecific Molecule Targeting CD40 and Tumor Antigen Mesothelin enhances tumor-specific immunity. Cancer Immunol Res. 2019;7(11):1864–75.
46. Luke JJ et al. Phase I study of ABBV-428, a mesothelin-CD40 bispecific, in patients with advanced solid tumors. J Immunother Cancer, 2021. 9(2).
47. Chiu D, et al. A PSMA-Targeting CD3 bispecific antibody induces antitumor responses that are enhanced by 4-1BB Costimulation. Cancer Immunol Res. 2020;8(5):596–608.
48. Wei H, et al. Dual targeting of CD137 co-stimulatory and PD-1 co-inhibitory molecules for ovarian cancer immunotherapy. Oncoimmunology. 2014;3:e28248.
49. Azpilikueta A, et al. Successful immunotherapy against a Transplantable Mouse Squamous Lung Carcinoma with Anti-PD-1 and Anti-CD137 monoclonal antibodies. J Thorac Oncol. 2016;11(4):524–36.
50. Claus C et al. Tumor-targeted 4-1BB agonists for combination with T cell bispecific antibodies as off-the-shelf therapy. Sci Transl Med, 2019. 11(496).
51. Morello A, Sadelain M, Adusumilli PS. Mesothelin-targeted CARs: driving T cells to solid tumors. Cancer Discov. 2016;6(2):133–46.
52. Haas AR, et al. Phase I study of Lentiviral-Transduced Chimeric Antigen Receptor-Modified T Cells Recognizing Mesothelin in Advanced Solid cancers. Mol Ther. 2019;27(11):1919–29.

Publisher's note